Received: 4 July 2017 | Revised: 6 September 2017 | Accepted: 12 September 2017

DOI: 10.1002/sia.6328

WILEY SURFACE and INTERFACE ANALYSIS

RESEARCH ARTICLE

50 keV H^+ ion beam irradiation of Al doped ZnO thin films: Studies of radiation stability for device applications

Susanta Kumar Sahoo[1] | Sutanu Mangal[1] | D.K. Mishra[2] | Udai P. Singh[3] | Pravin Kumar[4]

[1] School of Applied Sciences, KIIT University, Bhubaneswar, 751024, Odisha, India

[2] Department of Physics, Faculty of Engineering and Technology (ITER), Siksha 'O' Anusandhan University, Bhubaneswar, 751030, Odisha, India

[3] School of Electronics Engineering, KIIT University, Bhubaneswar, 751024, Odisha, India

[4] Inter University Accelerator Centre, Aruna Asaf Ali Marg, New Delhi 110067, India

Correspondence
Pravin Kumar, Inter University Accelerator Centre, Aruna Asaf Ali Marg, New Delhi 110067, India.
Email: vishakhapk@gmail.com

Thin films of Al doped ZnO (Al:ZnO) were deposited on two substrates (Si and glass) at room temperature and 300°C using DC magnetron sputtering. These films were bombarded with 50 keV H^+ beam at several fluences. The pristine and ion beam irradiated films were analysed by X-ray diffraction, Raman spectroscopy, scanning electron microscopy, and UV-Vis spectroscopy. The X-ray diffraction analysis, Hall measurements, Raman and UV-Vis spectroscopy confirm that the structural and transport properties of Al:ZnO films do not change substantially with beam irradiation at chosen fluences. However, in comparison to film deposited at room temperature, the Al:ZnO thin film deposited at 300°C shows increased transmittance (from 70% to approximately 90%) with ion beam irradiation at highest fluence. The studies of surface morphology by scanning electron microscopy reveal that the ion irradiation yields smoothening of the films, which also increases with ion fluences. The films deposited at elevated temperature are smoother than those deposited at room temperature. In the paper, we discuss the interaction of 50 keV H^+ ions with Al:ZnO films in terms of radiation stability in devices.

KEYWORDS

Al doped ZnO, band gap, ion irradiation, SEM, thin films, UV-Vis, XRD

1 | INTRODUCTION

The ZnO is a wide band gap II – VI group semiconductor, which is commonly used in fabricating solar cells, flat panel displays, transparent high power electronics, light emitting diodes, gas sensors, and in several others power-operated new technology-based devices/components because of its excellent material properties viz low resistivity, high transmittance, and high exciton binding energy (60 meV) with good chemical and thermal stability.[1-5] The electron transport properties in semiconductors can be tuned by doping.[6] The literature studies show that Al has been a promising group-III dopant for ZnO to explore its applications further.[7,8] The ZnO thin film grown on a substrate shows signature of inherent defects due to various reasons. These defects can be annealed by depositing the films at elevated temperature. The substrate temperature helps in reducing the stress due to lattice mismatch and also allows the adatoms to diffuse uniformly on the surface. Further, influence of surface temperature on carrier concentration, crystalinity, optical transmission, band gap, etc has also been reported.[9-12]

The ion beams erode the materials surface, allow surface atoms to migrate because of energy deposited by losses, and create point/columnar defects in the bulk. Therefore, the morphological and structural changes in the materials can be introduced by the time-dependent bombardment of various ion beams tuned properly in the energy, mass, flux, etc.[13] The dynamic annealing of defects during beam irradiation/exposure also plays major role in yielding the final state of the materials as far as such modifications are concerned.[14,15]

The ion beam modifications in the materials, if they are substantial, may change the response of the devices fabricated with these materials, and hence, the failure of the control system integrated with these. The success of the space programmes, which involve huge budget, human resources, and large time scales, depends on the radiation stability of the electronic devices used in the shuttles for a precise control.[16] The light ions such as hydrogen and helium are abundant in the space radiation (mainly Van Allen belts, plasma filling), and their exposure to a control device may degrade its performance.[17] Also, the cold ionospheric ions (H^+, H_2^+, O^+, and O_2^+) dominate the plasma escape from Mars. Adding the total outflow of hydrogen and oxygen respectively, the H/O ratio[18] may vary from 0.6 to 1.3. Therefore, it is quite important exercise to study the radiation stability of the electronic device fabricating materials against the exposure of light ions (such as H and He) in appropriate energy range. To further justify the choice of projectile ions in the present experiment, the irradiation of heavy or heavy inert ions (such as Ar, Kr,

and Xe) leads to the deposition of relatively higher nuclear energy in the materials without introducing any external chemical effect. The elastic collisions via nuclear energy losses produce point defects in the materials tailoring their properties for a specific application which is entirely a different research interest. The typical energy of the electrons and the protons in plasma filling space is ~50 to 100 keV with a flux of approximately 10^{12} cm^{-2} s^{-1}. Therefore, we irradiated 50 keV H^+ ion beam on Al:ZnO thin films at various fluence and studied the morphological changes and transport properties of the samples. Finally, we discussed the experimental results based on the understanding of ion-matter interactions.

2 | EXPERIMENTAL

The DC magnetron sputtering technique was used to deposit Al:ZnO thin films on 2 substrates: Si (n-type, Sb doped with the resistivity value of 0.008 Ω cm) and glass. Before film deposition, the substrate surfaces were properly cleaned. The Si surfaces were etched in a mixture of acids (HF: CH_3COOH: HNO_3:: 2: 3: 6) followed by ultrasonic cleaning with deionized water and iso-propanol. The glass surfaces were washed in a soap solution and then dried by blowing the N_2 gas. The sputtering chamber was thoroughly cleaned to achieve a base pressure of approximately 9.0 × 10^{-6} mbar with the targets placed inside it. Then the argon gas was injected in the sputtering chamber to maintain a working pressure of approximately 3.0 × 10^{-3} mbar. The sputtering was done at 400 W with 20 rpm of the substrate. The films were deposited by keeping the substrate at room temperature and also at 300°C. For sputtering, a commercially available target of ZnO (3 inches in diameter and 2 mm in thickness) with 2% Al was used. The thicknesses of the films were measured by Filmetrics F-10 thin film analyzer. For all samples, the measured film thickness was 150 ± 5 nm. These films were irradiated with 50 keV H^+ ion beam at 3 different fluences viz 1 × 10^{12}, 1 × 10^{13}, and 1 × 10^{14} ions/cm^2 using the low-energy ion beam facility[19] at Inter University Accelerator Centre (IUAC), New Delhi, India. During irradiation, the beam current on the samples was approximately 0.5 μA. The beam energy was chosen to meet real situation in the space environment. The ion range and straggling were deduced from Stopping of Ions in Matter (SRIM) 2008 software.[20] For the density of 5.67 g/cm^3, the stopping range of 50 keV H^+ ions in ZnO is 350.9 nm. The longitudinal and lateral straggling are 95.5 and 100.6 nm, respectively. The electronic energy loss (15.23 eV/Å) dominates over the nuclear energy loss (0.0624 eV/Å). The X-ray diffraction (XRD) analysis, Raman spectroscopy, UV-Vis spectroscopy, scanning electron microscopy (SEM), and

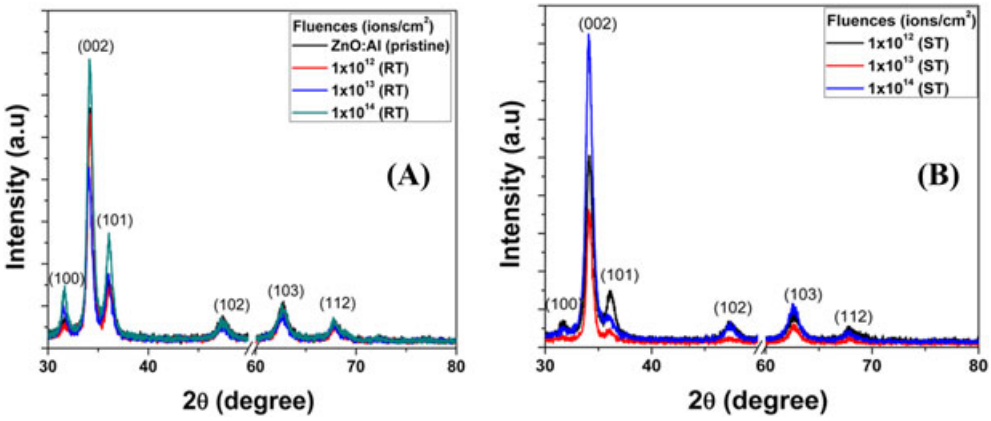

FIGURE 1 X-ray diffraction of the ion-irradiated (at various fluences) Al doped ZnO films; A, prepared at room temperature (RT); B, prepared at surface temperature of 300°C (ST)

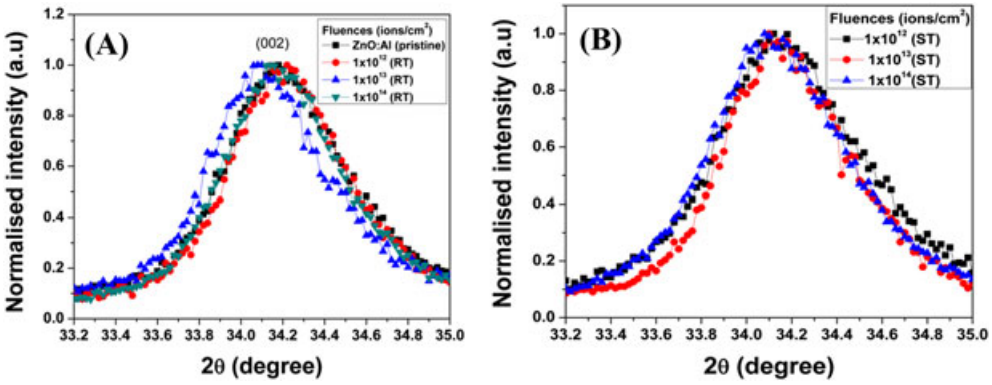

FIGURE 2 Zoom images of X-ray diffraction (002) peak of the ion-irradiated (at various fluences) Al doped ZnO films; A, prepared at room temperature (RT); B, prepared at surface temperature of 300°C (ST)

Hall measurements of ion beam irradiated films were performed to study surface morphology and structural, electrical, and optical properties. The silicon, which is quite suitable substrate for the transport measurements on ZnO films because of its conductivity, is opaque to UV-Vis photons making the optical measurements difficult in transmission mode. Therefore, the films deposited on the glass substrate were used for the optical measurements. In figures showing measurements, RT and ST abbreviations have been used for the films deposited at room temperature and at elevated surface temperature of 300°C, respectively.

TABLE 1 Analysis of X-ray diffraction (002) peak of Al doped pristine and ion-irradiated ZnO films

Fluence (ions/cm^2)	FWHM (degree)	Lattice Parameter (A^0)	c/a
Al-ZnO (pristine)	0.7	a = 3.257 c = 5.240	1.60
1×10^{12}(RT)	0.7	a = 3.246 c = 5.234	1.61
1×10^{13}(RT)	0.7	a = 3.274 c = 5.252	1.60
1×10^{14}(RT)	0.7	a = 3.258 c = 5.244	1.60
1×10^{12}(ST)	0.8	a = 3.265 c = 5.249	1.60
1×10^{13}(ST)	0.7	a = 3.263 c = 5.252	1.60
1×10^{14}(ST)	0.7	a = 3.254 c = 5.249	1.61

Note: RT stands for films, which are prepared at room temperature, and ST stands for films, which are prepared at elevated surface temperature of 300°C.

3 | RESULT AND DISCUSSION

The XRD patterns of 50 keV H^+ ion beam irradiated Al doped ZnO thin films deposited at room temperature (RT) and 300°C surface temperature (ST) are shown in Figure 1A,B, respectively. The patterns suggest that the films have wurtzite hexagonal polycrystalline ZnO structure, which is also confirmed from JCPDS #790208 data file. All films are c-axis oriented with prominent (002) peak due to self-ordering effect[21] to minimize the surface free energy. The irradiation at highest fluence yielded improved crystalinity of the films. The normalized (002) peak of the pristine and ion-irradiated Al:ZnO films deposited at room temperature and 300°C is shown in Figure 2A,B, respectively. The analysis of (002) peak at various temperature conditions is summarized in Table 1. It can be noticed that FWHM of the peak and lattice parameters remain almost unchanged indicating no major changes in the crystal structure of ZnO upon irradiating it with 50 keV H^+ ion beam at different fluences. To get further information on structural modifications, Williamson-Hall plots[22,23] of all samples have been drawn and are shown in Figures 3 and 4, respectively. The method takes care of individual contribution of XRD peaks in determining average crystallite size and lattice strain. The slope and intercept of the plot between βcosθ and 4sinθ

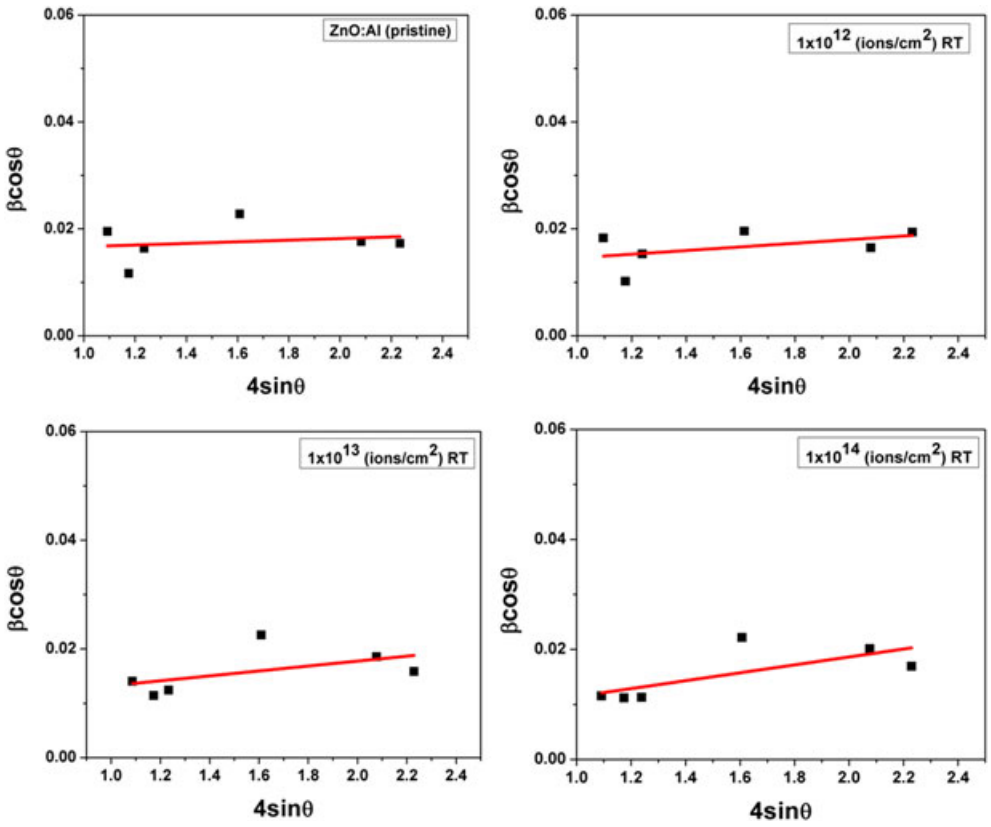

FIGURE 3 Williamson-Hall plots of Al doped ZnO films prepared at room temperature (RT) and irradiated with 50 keV H^+ ion beam with different fluences

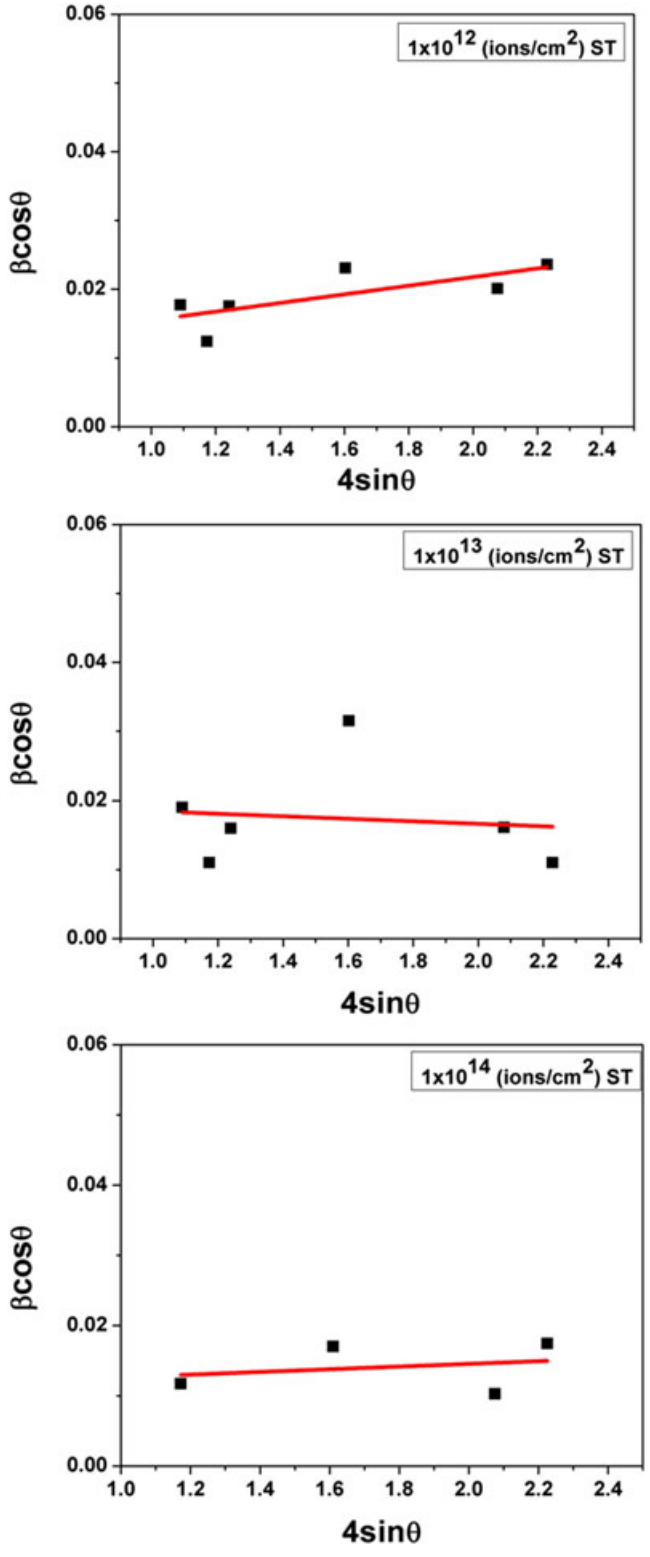

FIGURE 4 Williamson-Hall plots of Al doped ZnO films prepared at elevated temperature of 300°C and irradiated with 50 keV H^+ ion beam with different fluences

(where β is FWHM of the XRD peaks) provide lattice strain and crystallite size of the film, respectively.[24] The analysis of Williamson-Hall plots is summarized in Table 2. For films deposited at room temperature, the crystallite size and strain are found to be increased with the ion fluence. However, the variation of these parameters with ion fluence shows a very peculiar behaviour for the films deposited

TABLE 2 Analysis of Williamson-Hall plots of Al doped pristine and ion-irradiated ZnO films

Fluence (ions/cm^2)	Crystallite Size (nm)	Strain
Al-ZnO (pristine)	9.04 ± 2.5	0.0015 ± 0.003
1 × 10^{12}(RT)	12.19 ± 3.8	0.0033 ± 0.003
1 × 10^{13}(RT)	15.77 ± 6.3	0.0045 ± 0.003
1 × 10^{14}(RT)	32.24 ± 18.8	0.0071 ± 0.003
1 × 10^{12}(ST)	14.86 ± 5.0	0.0062 ± 0.002
1 × 10^{13}(ST)	6.74 ± 2.5	−0.0018 ± 0.007
1 × 10^{14}(ST)	12.79 ± 5.8	0.0019 ± 0.005

RT stands for films, which are prepared at room temperature, and ST stands for films, which are prepared at elevated surface temperature of 300°C.

at elevated temperature of 300°C. With increasing fluence, the crystallite size decreases for intermediate fluence and increases again at highest fluence. The strain also decreases. At intermediate fluence, the signature of compressive strain is noticed. At highest fluence, the films deposited at elevated temperature show relatively lower strain and crystallite size. The c/a ratio remains almost unchanged further confirming no major structural modifications. Depending upon initial microstructure of the thin films, the ion beam irradiation can lead to grain growth via Ostwald ripening[25] or dissolution of grains via kinetic/electronic sputtering. The local heating due to electronic energy losses can either yield to merging of the grain boundaries[26] or dissolution of bigger grains by various sputtering processes.[27] The ZnO films deposited at room temperature are of smaller grains, and therefore, ion impact meets several grain boundaries, which are annihilated because of local heating produced due to ion energy losses. The bigger grains in the films deposited at elevated temperature undergo for the sputtering upon ion irradiation, and hence, those are dissolved. To complete high fluences, the ion beam is continuously bombarded on target for large time scales. The local heating of the sample due to beam power again yields the agglomeration of smaller grains at high fluence.

The Raman spectra of Al doped ZnO thin films are shown in Figure 5. Most intense peak appeared at 520 cm^{-1} is because of

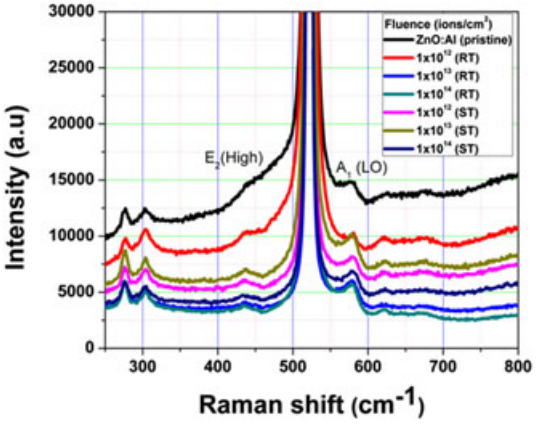

FIGURE 5 Raman spectra of the pristine and the ion-irradiated (at various fluences) Al doped ZnO films prepared at room temperature (RT) and at surface temperature of 300°C (ST)

Si substrate. The peak observed at 437 cm^{-1} is the characteristic of wurtzite hexagonal structure of ZnO and corresponds to non-polar E_2 (high) mode, which involves mainly vibration of oxygen atoms perpendicular to c-axis. Other non-polar E_2 (low) mode arising due to the vibration of Zn atoms appears at 99 cm^{-1}, which is not shown in the figure. The polar E_1 and A_1 oxygen-dominated phonons have LO and TO components (A_1 [TO] at 380 cm^{-1}, A_1 [LO] at 574 cm^{-1}, E_1 [TO] at 407 cm^{-1}, E_1 [LO] at 583 cm^{-1}).[28] Both E_1 and A_1 (TO) modes are probably suppressed because of thin film nature of the materials. The peak observed at 570 to 580 cm^{-1} represents structural disorder like oxygen vacancies, Zn interstitials, and the combinations of both. The other peaks observed at 275 and 302 cm^{-1} correspond to B_1 (low) silent mode of wurtzite ZnO and second-order E_2 (high) to E_1 (low) mode, respectively. With increasing ion fluence, both types of films do not show evolution of any other peak in the spectra confirming no major structural changes in Al:ZnO. However, E_2 (high) mode in films deposited at room temperature changes from a shoulder like feature to a more symmetric peak, which could be attributed to better film quality as also confirmed from XRD results.

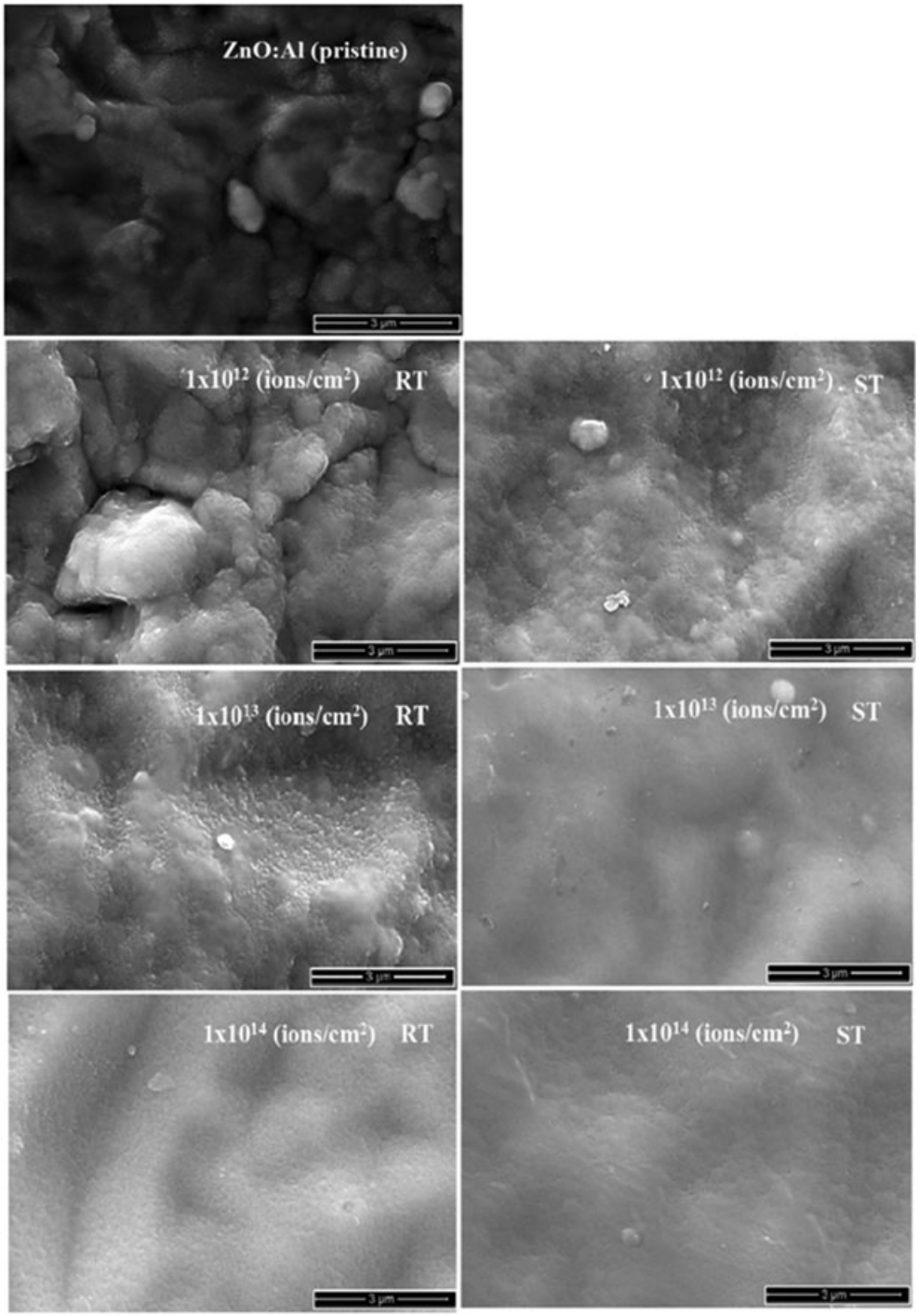

FIGURE 6 Scanning electron microscopy micrographs of the pristine and the ion-irradiated (at various fluences) Al doped ZnO films prepared at room temperature (RT) and at surface temperature of 300°C (ST)

The surface morphology of the pristine and 50 keV H^+ ion beam irradiated Al doped ZnO as probed by SEM is shown in Figure 6. It can be clearly seen that 2 types of films undergo surface smoothening upon ion irradiation. The smoothing increases with the ion fluence, and films deposited at elevated temperature of 300°C are relatively smoother with irradiation at constant fluence. The lightest H^+ ions upon impinging on Al:ZnO surface will certainly be backscattered. Therefore, the sputtering yield would be quite low compared to backscattering yield resulting in the surface smoothening[29,30] (rather than coarsening). The local surface heating due to the electronic energy losses (elastic collisions are negligible as seen by SRIM calculations) by the ion beam also helps in diffusion of atoms on the surface causing further smoothening.

Al:ZnO thin films deposited only on glass substrate and irradiated at different fluences were used to study the optical properties. Figure 7A,B shows the optical transmittance (in the wavelength range of 300-900 nm) of ion-irradiated Al:ZnO thin films deposited at room temperature and at 300°C. The films deposited at room temperature and irradiated with ion beam at different fluence show approximately 65% transmittance in the visible range. An enhanced transmittance value of approximately 90% is noticed for the ion beam–irradiated Al:ZnO thin films deposited at 300°C substrate temperature. With these results, we conclude that the deposition at elevated temperature yields better quality of Al:ZnO films and 50 KeV H^+ ion beam irradiation at chosen fluences does not affect the film quality much in terms of defects.

The relation between absorption coefficient (A) and band gap (E_g) of the material with the incident photon energy hv is $(Ahv)^2 = B(hv-E_g)$, where B is constant.[31] The direct band gap of semiconductor can be determined by drawing the tangent on the linear part of the graph between $(Ahv)^2$ and photon energy (hv) (Tauc plots; as shown in Figure 8A,B, respectively). The intercept by the tangent on X-axis provides the band gap. The band gap of the films deposited at room temperature and at 300°C was found to be 3.2 and 3.3 eV, respectively. No significant change in the band gap of 2 types of films has been observed with the ion irradiation even at higher fluences. The transport properties of Al doped ZnO films deduced from Hall measurements are shown in Table 3. All films deposited at 2 temperature conditions and irradiated with 50 KeV H^+ ion beam at 3 different fluences show resistivity in the range of mΩ-cm and a carrier concentration value of approximately $10^{21}/cm^3$. The enhanced mobility in the films deposited at elevated temperature is attributed to better quality of the films arising due to thermal annealing of the defects during deposition.

As seen from SRIM calculations, the nuclear energy loss for 50 KeV H^+ ion beam irradiation on Al:ZnO is negligible. Therefore, we expect absence of the elastic collisions (which are responsible for point defects) in the material. The electronic energy loss for this

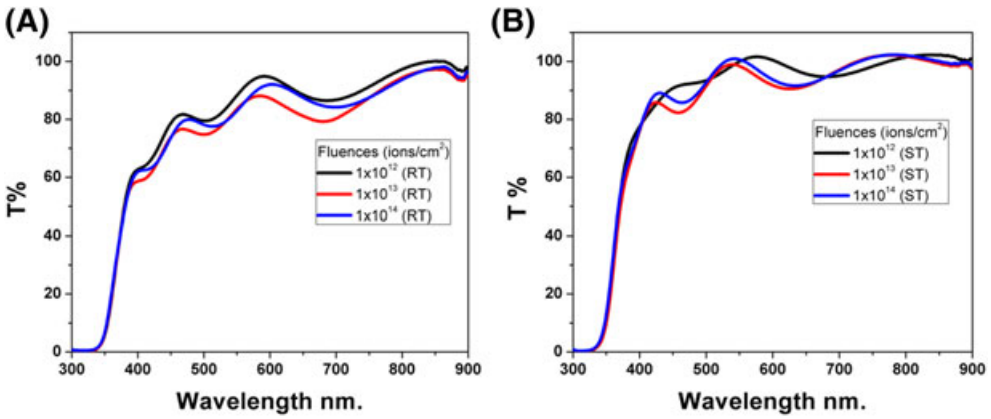

FIGURE 7 Transmission spectra of the ion-irradiated (at various fluences) Al doped ZnO films; A, prepared at room temperature (RT); B, prepared at surface temperature of 300°C (ST)

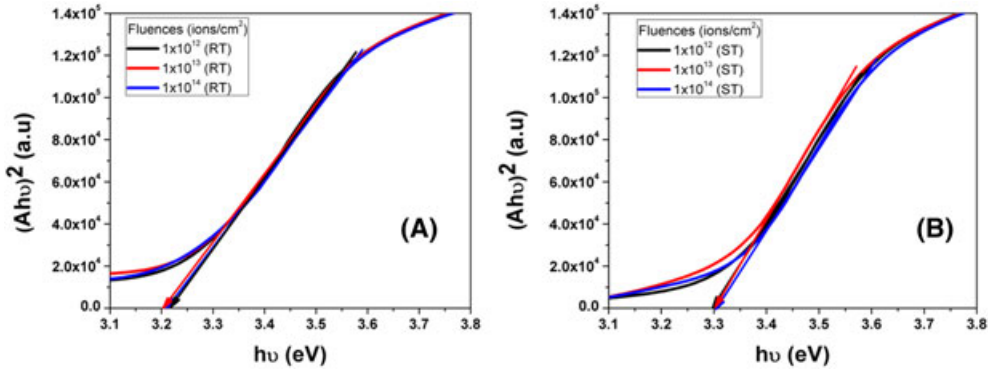

FIGURE 8 Tauc plots of the ion-irradiated (at various fluences) Al doped ZnO films; A, prepared at room temperature (RT); B, prepared at surface temperature of 300°C (ST)

TABLE 3 Hall measurements of Al doped pristine and ion-irradiated ZnO films

Fluence (ions/cm^2)	Carrier Conc (cm^{-3})	Resistivity (Ohm cm)
Al-ZnO	1.814E + 21	3.143E-03
1×10^{12}(RT)	1.816E + 21	1.601E-03
1×10^{13}(RT)	1.183E + 21	4.579E-03
1×10^{14}(RT)	1.166E + 21	3.138E-03
1×10^{12}(ST)	9.732E + 20	1.776E-03
1×10^{13}(ST)	1.105E + 21	1.372E-03
1×10^{14}(ST)	8.450E + 20	1.658E-03

RT stands for films, which are prepared at room temperature, and ST stands for films, which are prepared at elevated surface temperature of 300°C.

projectile-target combination is not substantial to generate thermal spikes in the materials to yield columnar defects.[32] Doping of Al in ZnO helps in dissipating the local heat produced by the ion beams and further minimize the possibility of temperature spike upon ion impact. However, the local temperature rise in the material during ion irradiation is sufficient to promote grain growth and the diffusion of surface atoms, and this could be the reason for changes only in the crystallite size and surface smoothening of samples upon ion beam bombardment. The crystal structure and optical and transport properties of films remain almost unaffected upon 50 keV H^+ beam irradiation at chosen fluences because of absence of point defects. Furthermore, it is deduced from SRIM calculations that only 0.03% of the total energy loss by 50 keV H^+ ions in Al:ZnO is responsible for vacancies production. A large fraction of the energy loss (approximately 98%) causes ionization/excitations. Without producing substantial point defects (vacancies/interstitials) and lattice distortion, we cannot expect any structural change and subsequent band gap engineering via origin of optically active defect levels in the target. Therefore, we can conclude that Al:ZnO shows radiation stability against present ion beam irradiation conditions.

4 | CONCLUSION

The Al:ZnO thin films deposited on 2 substrates (Si and glass) placed at 2 temperature conditions (RT and 300°C) were irradiated with 50 keV H^+ ion beam. The ion beam irradiation was done at 3 different fluences viz 1×10^{12}, 1×10^{13}, and 1×10^{14} ions/cm^2. The analysis of XRD patterns confirmed the wurtzite hexagonal polycrystalline nature of the films, and no substantial changes in the crystal structure of Al:ZnO were noticed upon ion irradiation. However, with increasing ion fluences, the crystallinity of the films improved and crystallite size also changed as confirmed by Williamson-Hall plots. Raman measurements also showed radiation stability of the films. The SEM micrographs revealed that ion irradiation yielded surface smoothening of the films. The transport properties (such as carrier concentration, and resistivity) and optical properties (such as transmittance and band gap) of the films remained unaffected with the ion irradiation. The films deposited at elevated temperature showed better quality (crystallinity and smoother surface), higher optical transmittance (approximately 90%), and a bit larger band gap (3.3 eV). The stability of Al:ZnO films against proton radiation is an interesting fact to realize its applications in optoelectronic devices for space programmes.

ACKNOWLEDGEMENTS

One of the authors (SKS) thanks Dr Fouran Singh, senior scientist, IUAC, New Delhi, for Raman measurements and Moserbaer India Ltd for providing SEM facility.

ORCID

D.K. Mishra http://orcid.org/0000-0002-5648-8362
Pravin Kumar http://orcid.org/0000-0002-6167-2535

REFERENCES

1. Özgür Ü, Alivov YI, Liu C, et al. A comprehensive review of ZnO materials and devices. *J Appl Phys*. 2005;98(4):041301.
2. Fernandez S, Naranjo FB. Optimization of aluminum-doped zinc oxide films deposited at low temperature by radio-frequency sputtering on flexible substrates for solar cell applications. *Solar Energy Materials and Solar Cells*. 2010;94(2):157.
3. Chae GS. A modified transparent conducting oxide for flat panel displays only. *Jpn J Appl Phys*. 2001;40(3R):1282.
4. Suchea M, Christoulakis S, Moschovis K, Katsarakis N, Kiriakidis G. ZnO transparent thin films for gas sensor applications. *Thin Solid Films*. 2006;515(2):551.
5. Sun XW, Huang JZ, Wang JX, Xu Z. A ZnO nanorod inorganic/organic heterostructure light-emitting diode emitting at 342 nm. *Nano Lett*. 2008;8(4):1219.
6. Kim KK, Reina A, Shi Y, et al. Enhancing the conductivity of transparent graphene films via doping. *Nanotechnology*. 2010;21(28):285205.
7. Sernelius BE, Berggren KF, Jin ZC, Hamberg I, Granqvist CG. Band-gap tailoring of ZnO by means of heavy Al doping. *Physical Review B*. 1988;37(17):10244.
8. Lee JH, Park BO. Characteristics of Al-doped ZnO thin films obtained by ultrasonic spray pyrolysis: effects of Al doping and an annealing treatment. *Materials Science and Engineering: B*. 2004;106(3):242-245.
9. Ondo-Ndong R, Pascal-Delannoy F, Boyer A, Giani A, Foucaran A. Structural properties of zinc oxide thin films prepared by r.f. magnetron sputtering. *Mater Sci Eng B*. 2003;97:68.
10. Son CS, Kim SM, Kim YH, et al. Deposition temperature dependence of Zno/Si grown by pulsed laser deposition. *J Korean Phys Soc*. 2004;45:685.
11. Cho S. Structural and optical properties of ZnO films grown on sapphire substrates subjected to substrate temperature. *J Korean Phys Soc*. 2006;49:985.
12. Zhu L, Ye Z, Zhuge F, Yuan G, Lu J. Al–N codoping and p-type conductivity in ZnO using different nitrogen sources. *Surf Coat Technol*. 2005;198:354.
13. Jain IP, Jain G. Ion beam induced surface and interface engineering. *Surf Sci Rep*. 2011;66(3):77.
14. Kucheyev SO, Williams JS, Jagadish C, et al. Ion-beam-produced structural defects in ZnO. *Physical Review B*. 2003;67(9):094115.
15. Lorenz K, Alves E, Wendler E, Bilani O, Wesch W, Hayes M. Damage formation and annealing at low temperatures in ion implanted ZnO. *Appl Phys Lett*. 2005;87(19):191904.
16. Ryu YR, Lee TS, Lubguban JA, White HW, Park YS, Youn C. ZnO devices: photodiodes and p-type field-effect transistors. *Appl Phys Lett*. 2005;87(15):153504.
17. Srour JR, McGarrity JM. Radiation effects on microelectronics in space. *Proc IEEE*. 1988;76(11):1443-1469.

18. Lundin R, Barabash S, Holmstro M, et al. Atmospheric origin of cold ion escape from Mars. *Geophys Res Lett*. 2009;36:L17202.

19. Kumar P, Rodrigues G, Rao UK, Safvan CP, Kanjilal D, Roy A. ECR ion source based low energy ion beam facility. *Pramana–J Phys*. 2002;59(5):805.

20. Ziegler JF, Biersak JP, Littmark U. *Stopping and Range of Ions in Solids*. Pergamon, New York (new edition in 1996); 1985.

21. Lee HW, Lau SP, Wang YG, Tse KY, Hng HH, Tay BK. Structural, electrical and optical properties of Al-doped ZnO thin films prepared by filtered cathodic vacuum arc technique. *J Cryst Growth*. 2004;268(3):596-601.

22. Zak AK, Majid WA, Abrishami ME, Yousefi R. X-ray analysis of ZnO nanoparticles by Williamson–Hall and size–strain plot methods. *Solid State Sci*. 2011;13(1):251-256.

23. Biju V, Sugathan N, Vrinda V, Salini SL. Estimation of lattice strain in nanocrystalline silver from X-ray diffraction line broadening. *J Mater Sci*. 2008;43(4):1175-1179.

24. Thool GS, Singh AK, Singh RS, Gupta A, Susan MABH. Facile synthesis of flat crystal ZnO thin films by solution growth method: a micro-structural investigation. *J Saudi Chem Soc*. 2014;18(5):712-721.

25. Voorhees PW. The theory of Ostwald ripening. *Journal of Statistical Physics*. 1985;38(1):231-252.

26. Lovinger AJ, Forrest SR, Kaplan ML, Schmidt PH, Venkatesan T. Structural and morphological investigation of the development of electrical conductivity in ion-irradiated thin films of an organic material. *J Appl Phys*. 1984;55(2):476-482.

27. Sun AC, Yuan FT, Hsu J-H, Liao WM, Lee HY. Effect of bombardment with different ions (H, He, Ar) on ordering transformation of Fe 48 Pt 52 films. *J Appl Phys*. 2009;105:07B719.

28. Koyano M, QuocBao P, ThanhBinh L t, HongHa L, NgocLong N, Katayama S'i. Photoluminescence and Raman spectra of ZnO thin films by charged liquid cluster beam technique. *Phys Stat Sol A*. 2002;193(1):125-131.

29. Kumar P. Medium-energy ion irradiation of Si and Ge wafers: studies of surface nanopatterning and signature of recrystallization in 100 keV Kr^+ bombarded a-Si. *Semicond Sci Technol*. 2016;31:035014.

30. Hauffe W. Faceting mechanism in the sputtering process. *Phys Status Solidi A*. 1976;35:K93.

31. Riti Sethi, Priya Darshni Kaushik, Anver Aziz, Azher M. Siddiquia and Pravin Kumar. Ion induced controlled modifications in structural and optical properties of indium oxide thin films–studies with 25-keV Co^- and N^+ beam implantations. https://doi.org/10.1002/sia.6242

32. Wang ZG, Dufour C, Paumier E, Toulemonde M. The Se sensitivity of metals under swift-heavy-ion irradiation: a transient thermal process. *J Phys Condens Matter*. 1994;6(34):6733.

How to cite this article: Sahoo SK, Mangal S, Mishra DK, Singh UP, Kumar P. 50 keV H^+ ion beam irradiation of Al doped ZnO thin films: Studies of radiation stability for device applications. *Surf Interface Anal*. 2017;1–8. https://doi.org/10.1002/sia.6328